INTERNATIONAL JOURNAL OF Electroactive Materials

Int. J. Electroactive Mater. 4 (2016) 14 – 17
www.electroactmater.com

Short Communication

Structural, Electronic and Optical Properties of $BaTiO_3$ and $BaFeO_3$ From First Principles LDA+U Study

M.F.M. Taib[1, 4*], N.H. Hussin[1, 4], M.H. Samat[1, 4], O.H. Hassan[2, 4], M.Z.A. Yahya[3, 4]

[1]Faculty of Applied Sciences, Universiti Teknologi MARA 40450 Shah Alam,Selangor Malaysia
[2]Department of Industrial Ceramics, Faculty of Arts & Design, Universiti Teknologi MARA, 40450 Shah Alam, Selangor, Malaysia
[3]Department of Defence Science, Universiti Pertahanan Nasional Malaysia, 57000 Kuala Lumpur, Malaysia
[4]Ionic Materials and Devices (iMADE) Research Laboratory, Institute of Science, Universiti Teknologi MARA, 40450 Shah Alam, Selangor, Malaysia
E-mail Address: mfariz@salam.uitm.edu.my

Received: 18 November 2016 / Accepted: 7 December 2016 / Published: 9 December 2016

ABSTRACT: The first principles study based on density functional theory within local density approximation plus Hubbard U approach as implemented in Cambridge Serial Total Energy Package code has been used to investigate the structural, electronic and optical properties of cubic $BaTiO_3$ and $BaFeO_3$. We observed that the structural properties and band structures of cubic $BaTiO_3$ and $BaFeO_3$ changes when the LDA+U method was employed. Further study on the properties of the both structures were carried out with the calculation of density of states to show the hybridization between Fe-O, Ba-O and Ti-O. The comparison between $BaTiO_3$ and $BaFeO_3$ on the optical properties was discussed using the calculated optical absorption spectra. These results would provide a theoretical reference for fundamental science as well as technological application of $BaTiO_3$ and $BaFeO_3$.
Keywords: Density functional theory; First principles; Electronic properties; Optical properties; Structural properties

1. Introduction

Barium titanate ($BaTiO_3$) is a typical perovskite compound and it has been used for infrared sensors, electromechanical transducers and optical modulators as its large dielectric constant, and noticeable pyroelectric, piezoelectric and electro-optic effects [1-3]. The structure of the perfect $BaTiO_3$ has a cubic symmetry as paraelectric with space group of P*m3m* (no 221) [4]. Its lattice consists of corner-sharing oxygen octahedral with interpenetrating simple cubic lattices of Ba and Ti cations [5]. The Ti cations sit at the center of each one of the oxygen octahedrals, while the Ba ions lie in 12-fold coordinated sites between the octahedral. The properties of $BaTiO_3$ can be easily modified [6], for example, the Ba, Ti and O atoms can be replaced by other impurity atoms. The properties of $BaTiO_3$ and also $BaFeO_3$ have been extensively studied in both experimental and theoretical works.

Fuentes et al. [7] prepared $BaTiO_3$ powders using a sol-gel-hydrothermal process to study its effects at different times and calcination temperatures. Ali et al. [8] prepared La-doped $BaTiO_3$ thin films and studied the composition of the films. Polycrystalline $BiFeO_3$ thin films on ITO coated glass substrates were prepared and characterized by Park et al. [9] using pulsed laser deposition. Recently, Pugaczowa-Michalska and Kaczkowski [10] studied the effect of rare-earth-doped in $BaFeO_3$ which shows the increasing of magnetization as the number of *4f* electron increases. The comparison between $BaTiO_3$ and $BaZrO_3$ are studied by Khenata et al. [11] using the full-potential linear augmented plane wave (FP-LAPW) to investigate their properties. However, the comparison between $BaTiO_3$ and $BaFeO_3$ for their properties has not been further studied especially by using first principles study and the Hubbard U method.

In this paper, different with literatures, we studied the structural, electronic and optical properties of intrinsic $BaTiO_3$ and $BaFeO_3$ by using density functional theory (DFT) with local density approximation (LDA) plus Hubbard U approach. Theoretical computation studies based on ab-initio calculations can yield important information regarding the electrical and structural properties of these solids solution of $BaTiO_3$ and $BaFeO_3$. The work would be helpful for designing experiments and explaining the phenomenon in experimental study especially on the ground state structure and electronic and optical properties of materials.

2. Computational method

The first principles calculations were performed using density functional theory (DFT) as implemented in Cambridge Serial Total Energy Package (CASTEP) [12] computer code within local density approximation (LDA) by Ceperley and Adler [13] as parameterized by Perdew-Zunger [14] (CA-PZ) functional [5, 15, 16]. The first principles calculations of LDA+U method were applied using U = 4 eV as reported from the previous study [10]. The atomic crystal structures of cubic $BaTiO_3$ and $BaFeO_3$ used in this work are illustrated in **Figure 1** and **Figure 2** respectively. A plane-wave cut off energy with 340 eV and the Brillouin zone with the 4x4x4 k-point (converged) were applied. A stress threshold of 0.05 GPa was used for cell relaxation, and forces on ions were converged below 0.03 eV/Å. Ultrasoft pseudopotentials, a plane-wave basis

set, and a conjugate-gradients algorithm were used to compute the total energies and forces for the $BaTiO_3$ (BTO) and $BaFeO_3$ (BFO) crystal configurations. The method and the detail of pseudopotentials employed have been described elsewhere.

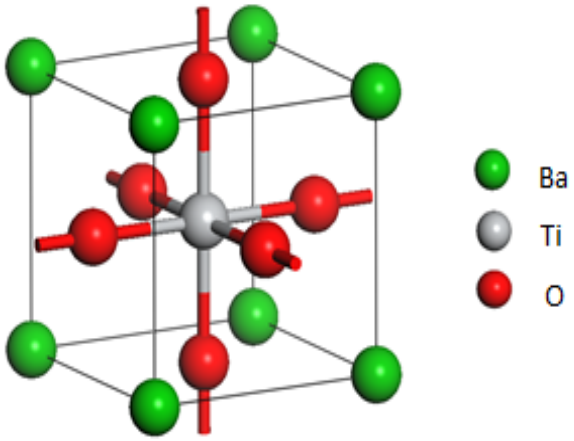

Figure 1: Crystal structure of $BaTiO_3$ unit cell

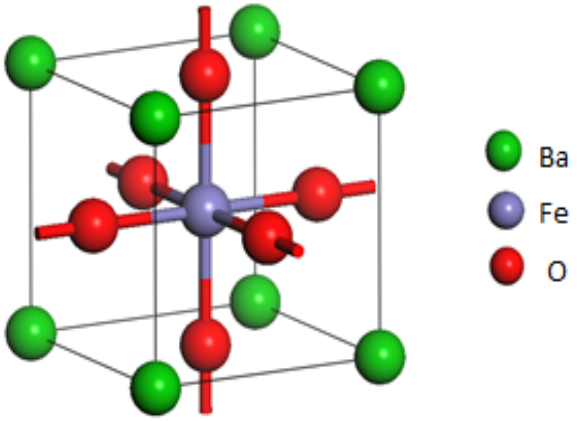

Figure 2: Crystal structure of $BaFeO_3$ unit cell

3. Results and discussions

3.1 Structural Properties of $BaTiO_3$ and $BaFeO_3$

The values of unit cell lattice parameter, volume and atomic bonding of BTO and BFO were optimized from the geometry optimization calculation as listed in **Table 1.** In this calculation, the structural optimizations of BTO and BFO with exchange correlations LDA+U (U = 4 eV) were utilized. It can be observed that the results obtained from this CASTEP computer code are in good agreement with the previous experimental study of BTO [17, 18]. The accurateness of the lattice calculation and its atomic position become a significant factor of the material stability and for further use in other calculations in perovskite oxide. Therefore, we should ensure that the structural calculation used is acceptable, although there is the lack study of BFO using first principles method. The reported BFO lattice parameters from experimental data [19] are in agreement with LDA+U obtained from this present work.

Table 1: Structural parameters of $BaTiO_3$ (BTO) and $BaFeO_3$ (BFO) in comparison with experimental work

	BTO	BTO	BFO	BFO
	LDA+U	Expt.[17]	LDA+U	Expt.[19]
a (Å)	3.954	4.012	3.892	3.97
V (Å^3)	61.80	63.57	58.97	62.57
Bi-O (Å)	2.796	3.355	2.752	-
Ti-O (Å)	1.977	3.791	-	-
Fe-O (Å)	-	-	1.946	-

3.2 Band Structures and Density of States of $BaTiO_3$ and $BaFeO_3$

The calculated electronic band structures along the direction of high-symmetry Brillouin zone for cubic BTO and BFO are shown in **Figure 3(a)** and **3(b)**, respectively. The highest valence band (VB), which lies at the Fermi level (E_F) at 0 eV is dominated by the O *2p* for both compounds. While the conduction band (CB) for BTO and BFO occurs at G point, which is primarily dominated by Ti *3d* and Fe *3d* electrons. The calculation of electronic band gap shows that BTO and BFO has an indirect band gap with the high value of 1.778 eV and 2.846 eV at R-G point, respectively. The experimental band gap is ~ 3.20 eV and 2.74 eV for BTO and BFO respectively [20, 21]. After corrected the band gap with U = 4 eV, the electronic properties of BTO and BFO increased with a better description on the localization of transition metal Ti *3d* and Fe *3d* electrons. This phenomenon is expected to happen due to the localization of *d*-states electron in the crystal system. The valence band above the 0 eV energy Fermi because the spin polarized were not considered during analysis (alpha and beta magnetic spin) by directly compared the total band structures between $BaTiO_3$ (BTO) and $BaFeO_3$ (BFO). In addition, the inclusion of U = 4 eV shift the Fe *3d* states above Fermi level at higher energy for BFO. Details of the electron density of materials will be explained in DOS section.

The partial and total density of states (DOS) for BTO and BFO are shown in **Figure 4(a)** and **4(b)**. The highest VBs is mainly dominated by electron O *2p* for all compositions of compounds and the lowest CBs is mainly originated from the Ti *3d* and Fe *3d* states. The separation between VBs and CBs for BTO and BFO is 1.778 eV and 2.846 eV, respectively, as obtained from the value of band gap. This is due to the different covalency strength of the Ba-O, Ti-O and Fe-O. The hybridization state of Ba, Fe, Ti and O also occurred as shown in DOS results.

3.3 Optical Properties of $BaTiO_3$ and $BaFeO_3$

The absorption spectra was calculated for BTO and BFO as shown in **Figure 5** and **Figure 6** in the photon energy and wavelength, respectively. The values of static absorption increased with photon energy in the transparency region (ultraviolet region) BTO and BFO. Subsequently, the value of absorption edge shows the

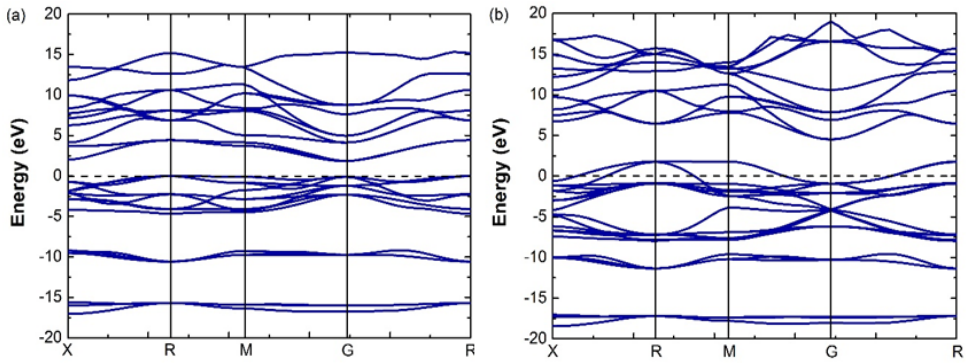

Figure 3: Band structures of (a) $BaTiO_3$ and (b) $BaFeO_3$ from LDA+U calculation

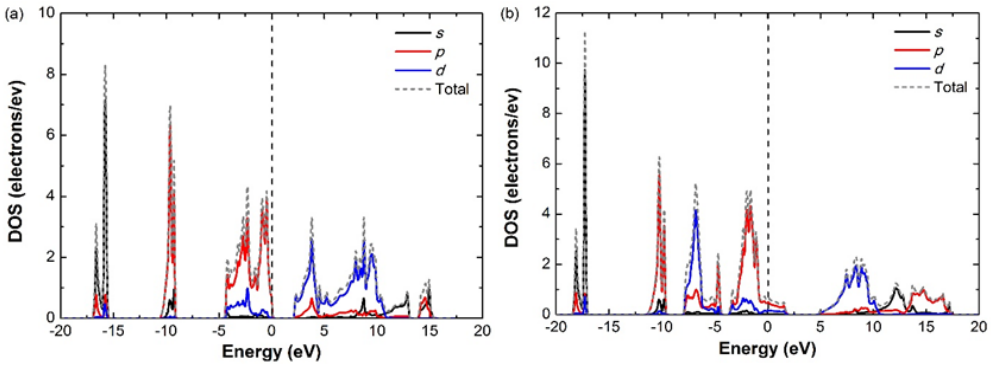

Figure 4: Density of states of a) $BaTiO_3$ and (b) $BaFeO_3$ from LDA+U calculation

trend as presented in electronic DOS in **Figure 4**. In this work, the absorption spectra correspond to the zero value for the real part ε_1 (ω) of the dielectric function. Since optical properties are closely related to the electronic band structure and phonon dispersion, therefore both types of inter-band optical transitions viz. direct band gap and indirect band gap can be calculated from the above information. The absorption edge spectra for BTO and BFO are observed to correspond with the calculated energy band gap as discussed in electronic part. The optical absorption involves the electrons transition from the highest VBs (dominated by O *2p* at point R) to the CBs, that have primary components from the Ti *3d* and Fe *3d* states. The absorption edge of BTO and BFO appeared in visible range at about 400 to 600 nm.

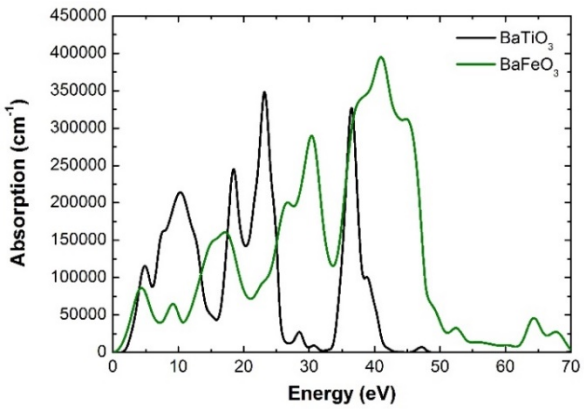

Figure 5: Absorption of $BaTiO_3$ and $BaFeO_3$ within range of photon energy

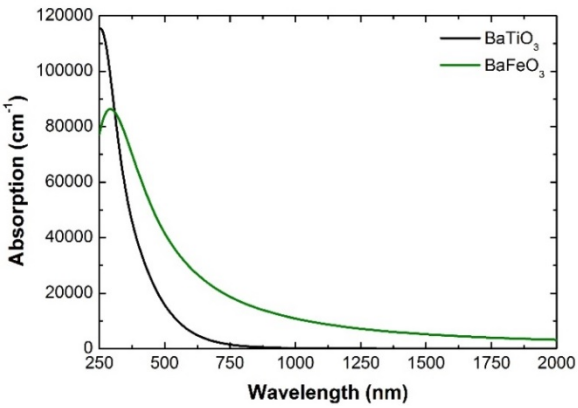

Figure 6: Absorption of $BaTiO_3$ and $BaFeO_3$ within range of wavelength

4. Conclusion

The calculated structural parameters, electronic and optical properties of the cubic BTO and BFO using the LDA+U functional are in a good agreement with the results reported in the experimental work. Thus, this work provided an accurate structural optimization for BTO and BFO using LDA+U functional. We have also successfully reported the relation between electronic and optical properties which could provide theoretical basis to other scholars as a reference in synthesizing those BTO and BFO materials.

Acknowledgements

The authors would like to acknowledge the Faculty of Applied Sciences, UiTM Malaysia for the facilities and

supports provided during the completion of this research. The authors also thank the Ministry of Education, Malaysia for the financial support with NRGS grant.

References

[1] K. Sutjarittangtham, N. Tawichai, U. Intatha, S. Eitssayeam, K. Pengpat, G. Rujijanagul, and T. Tunkasiri, AIP Conf. Proc. 1151 (2009) 174–176.

[2] B. Noheda, J. Gonzalo, L. Cross, R. Guo, S.-E. Park, D. Cox, and G. Shirane, Phys. Rev. B, 61 (2000) 8687–8695.

[3] M. Gröting and K. Albe, J. Solid State Chem., 213 (2014) 138–144.

[4] Y. X. Wang, M. Arai, T. Sasaki, C. L. Wang, W. L. Zhong, Surf. Sci., 585 (2005) 75–84.

[5] M. F. M. Taib, M. K. Yaakob, O. H. Hassan, and M. Z. A. Yahya, Integr. Ferroelectr., 142 (2013) 119–127.

[6] M. F. M. Taib, M. K. Yaakob, O. H. Hassan, A. Chandra, A. K. Arof, and M. Z. A. Yahya, Ceram. Int., 39 (2013) S297–S300.

[7] A. Fuentes, F. Cespedes, P. Munoz, E. Chavez, P.-C. Luis, J. Chil. Chem. Soc., 4 (2013) 2077–2081.

[8] A. I. Ali, K. Park, A. Ullah, R. Huh, and Y. S. Kim, Thin Solid Films, 551 (2014) 127–130.

[9] P. Jungmin, G. Fumiya, N. Seiji, K. Takeshi, and O. Masanori, J. Korean Phys. Soc., 59 (2011). 2537-2541.

[10] M. Pugaczowa-Michalska and J. Kaczkowski, J. Mater. Sci., 50 (2015) 6227–6235.

[11] R. Khenata, M. Sahnoun, H. Baltache, M. Rerat, A. H. Rashek, N. Illes, and B. Bouhafs, Solid State Commun., 136 (2005) 120–125.

[12] S. J. Clark, M. D. Segall, C. J. Pickard, P. J. Hasnip, M. I. J. Probert, K. Refson, M. C. Payne, Zeitschrift für Kristallographie, 220 (2005) 567–570.

[13] D. M. Ceperley and B. J. Alder, Phys. Rev. Lett., 45 (1980) 566–569.

[14] J. P. Perdew and A. Zunger, Phys. Rev. B, 23 (1981) 5048–5079.

[15] M. K. Yaakob, M. F. M. Taib, M. S. M. Deni, and M. Z. A. Yahya, Integr. Ferroelectr., 155 (2014) 134–142.

[16] A. Bouhemadou, R. Khenata, M. Chegaar, S. Maabed, Phys. Lett. A, 371 (2007) 337–343.

[17] G. H. Kwei, A. C. Lawson, S. J. L. Billinge, J. Phys. Chem. 97 (1993) 2368–2377.

[18] D. Bagayoko, G. L. Zhao, J. D. Fan, J. T. Wang, J. Phys. Condens. Matter, 10 (1998) 5645–5655.

[19] Z. Li, T. Iitaka, and T. Tohyama, Phys. Rev. B, 86 (2012) 1–5.

[20] S.H. Wample, M. Didomenico, I. Camlibel, J. Phys. Chem. Solids, 29 (1968)1797, 1968.

[21] S. Y. Yang, L. W. Martin, S. J. Byrnes, T. E. Conry, S. R. Basu, D. Paran, L. Reichertz, J. Ihlefeld, C. Adamo, A. Melville, Y. Chu, C. Yang, J. L. Musfeldt, D. G. Schlom, J. W. Ager, and R. Ramesh, Appl. Phys. Lett., 95 (2009) 062909-1–062909-3.